

Poorly Crystalline Ru_{0.4}Sn_{0.6}O₂ Nanocomposites Coated on Ti Substrate with High Pseudocapacitance for Electrochemical Supercapacitors

Yanqun Shao, Zhonghua Yi, Fenghua Lu, Fenyong Deng, Beibei Li

Institute for Materials Research, Fuzhou University, Fuzhou, China

Email: yqshao1989@163.com

Received September 21, 2011; revised October 28, 2011; accepted November 14, 2011

ABSTRACT

Poorly crystalline Ru_{0.4}Sn_{0.6}O₂ solid solution with size about 2 nm coated on Ti substrate was prepared by thermal decomposition at 260°C. The electrodes were characterized by X-ray diffraction (XRD), scanning electron microscopy (SEM) and transmission electron microscopy (TEM) for structural and morphological studies. The Capacitance properties of the electrodes were tested by cyclic voltammetry and charge-discharge tests. The results show that the electrodes have mud-cracks structure with cracks 0.2 μm in width. The electrode has stable electrochemical capacitor properties with a maximum specific capacitance of 648 F/g within a scan potential window -0.1 - 1.0 V in 0.5 M H₂SO₄ electrolyte solution.

Keywords: Specific Capacitance; Supercapacitor; RuO₂-SnO₂; Electrode; Thermal Decomposition

1. Introduction

Growing demands for power sources for transient high power density have stimulated great interest in electrochemical capacitors. Among them a chemical battery (supercapacitor) with large specific capacitance is rising. It has much advantage such as high power density, Faraday large electric capacity, high energy, wide range of operating temperatures, extremely long service life and environmental protection [1]. Supercapacitor usually divides into electric double layer capacitors (EDLC) and Faraday quasi-capacitors according to the type of reactions of electrodes [2]. EDLC is a small part of whole capacitance, on the other hand pseudocapacitance is a large part of it. The EDLC occurs in porous active carbon/fiber with very high specific surface area [3], whereas the pseudocapacitance is observed in transition metal oxides [4,5] (RuO₂ [4-10], IrO₂, MnO₂ [10-14], Co₃O₄ [15-17], NiO [18,19], SnO₂ [9] etc.) and conducting polymers [5]. So the electrode material is one of the key factors that decided the electrochemical capacitance [3]. A most successful electrode material is composed with RuO₂ due to the minimal energy requirements and oxide stability during proton diffusion into the crystal structure [4]. The highest capacitance of RuO₂ was reported of 380 F/g in the case of crystalline RuO₂ and 760 F/g in the case of hydrous RuO₂ with the bulk form [6]. Although pseudocapacitor has higher capacity than EDLC,

there are many disadvantages such as high raw material cost and process difficulty which limits its practical application. In order to overcome these disadvantages, some transition metal oxides which also characterize multivalent metal oxides are attracted to replace part of RuO₂. Highly stable RuO₂-Ta₂O₅/Ti electrodes with a specific capacitance of 170 F/gRuO₂⁻¹ and a lower capacitance (130 F/gRuO₂⁻¹) also are composed of crystalline RuO₂ and amorphous tantalum oxide [6]. So a fact can be concluded that a high capacitance must have an amorphous structure. SnO₂ is widely used as an additive in many catalysis fields because it is an inexpensive, environmentally friendly semiconductor material. For example adding SnO₂ to titanium anodes coatings can efficiently improve stability and the selectivity of chlorine reaction [9]. The author in literature [19] used two-step hydrothermal synthesis method to prepare Ru-Sn binary oxide electrodes, whose electric capacity reached to 1150 F/g. But only Ru-Sn oxide powder can be prepared first using this method. Carbon black and adhesive must be added to prepare coatings, which can produce side-effect of pseudocapacitance. Therefore, it is necessary to look for one-step method to prepare Ru-Sn oxide electrodes directly. This paper presented a method to prepare RuO₂-SnO₂ coatings directly on titanium substrate by thermal decomposition at low temperature. The structural, morphological, compositional and supercapacitance proper-

ties had been studied.

2. Experimental

Commercial RuCl_3 (36.9% Ru^{3+}) and SnCl_4 (98% Sn^{4+}) were used as the starting materials and the mole ratio of Ru^{3+} and Sn^{4+} was 4 to 6. The metal chlorides in the required proportions were each dissolved in a required amount of anhydrous ethanol ($\text{C}_2\text{H}_5\text{OH}$). They were mixed uniformly. The resultant solution was brushed onto the pretreated Ti substrate. The coatings were dried at 260°C in the oven for one hour.

X-ray diffraction (XRD: Rigaku, D/max Ultima III diffractometer with $\text{CuK}\alpha$ radiation) measurements were employed to investigate the crystallinity of the coatings. The scanning electron microscopy (SEM: HITACHI, S-4100) was performed to observe the surface. The transmission electron microscopy (TEM: JEOL-2000EX at 120 kV) was operated to analyze the microstructure. Electrochemical behaviors of the derived electrodes were examined using Cyclic voltammetry (CV) and galvanostatic charge-discharge in a 0.5 M H_2SO_4 electrolyte solution carried out in an electrochemical workstation (Auto Lab PGST-302A) at room temperature. Large area pure titanium plate was used as the counter electrode and saturated calomel electrode (SCE) as the reference electrode. CV test was performed between -100 and 1000 mV at a scan rate of $25 \text{ mV}\cdot\text{s}^{-1}$.

3. Results and Discussion

3.1. XRD Analysis

The XRD measurement was carried out to confirm the poor crystallinity of the as derived $\text{Ru}_{0.4}\text{Sn}_{0.6}\text{O}_2$ coatings. It's showed that the mixed oxides exhibit very broad and diffuse diffraction peaks. They can be due to poorly crystallized rutile phases. They are attributed not only to the RuO_2 and SnO_2 rutile-type oxide phase, but also to some new rutile-type oxide phases. These oxides show the strongest peaks with intermediate 2θ values between those of RuO_2 and SnO_2 , suggesting that these oxides must form a solid solution. The reflections in the pattern shift systematically to higher d -spacings than those of RuO_2 . It's indicated that tin is replaced by ruthenium according to the smaller ionic radius of the Ru^{4+} ion (0.76 \AA) with respect to Sn^{4+} (0.83 \AA), which is in agreement with the formation of solid solution phases with $(\text{Sn}, \text{Ru})\text{O}_2$ compositions. No metallic Ru phase was detected but one peak at about 40° which was corresponding to the Ti substrate (**Figure 1**).

3.2. SEM Analysis

SEM images of the coating surface at two magnifications are shown in **Figure 2**. It can be found that the electrodes

consist of mud-cracks structure and flat area. The area of each mud was also in the same size. The widths of the crack are about $0.2 \mu\text{m}$. Cracks can provide the space for the reaction of active RuO_2 and SnO_2 . It also provided the channel for the oxygen to result in the passivation of Ti substrate. Therefore, the cracks can deteriorate the electrochemical performance of as-prepared electrode. The flat areas of all the electrodes are composed of numerous nanosize particles which are not well-grown. Most of these particles are agglomerated to form flat area.

3.3. TEM Analysis

The HRTEM image is shown in **Figure 3**. The selected area diffraction (SAD) pattern shows that there is no any bright spot under illumination which confirms that formation of amorphous mixed oxide coating. But some small crystalline particles which are homogeneously distributed in the coatings can be seen clearly in **Figure 3(a)**. The sizes of these particles are about 1 - 3 nm. The EDS results show that this kind of particles consists of Ru, Sn, and O element (not shown here). Such type of morphology is different from not only the amorphous structure but also the crystalline structure. The amorphous structure is expected to have a high surface area which is

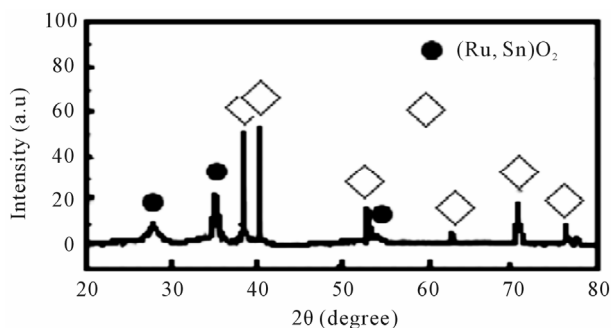


Figure 1. The XRD pattern of the $\text{Ti}/\text{Ru}_{0.4}\text{Sn}_{0.6}\text{O}_2$ electrode.

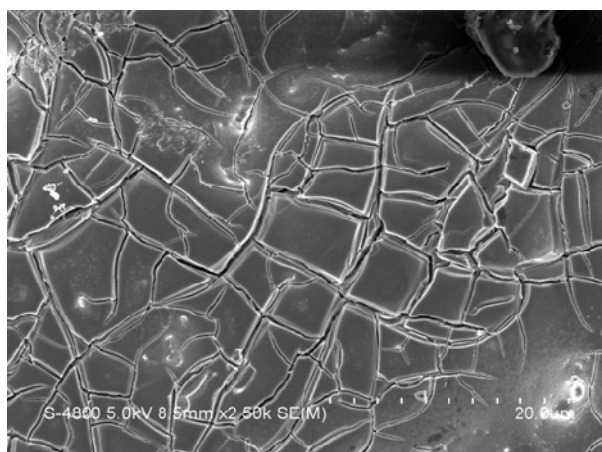
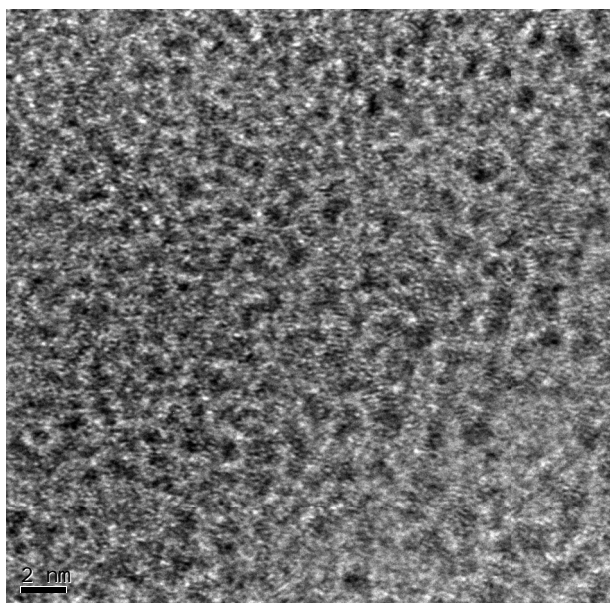
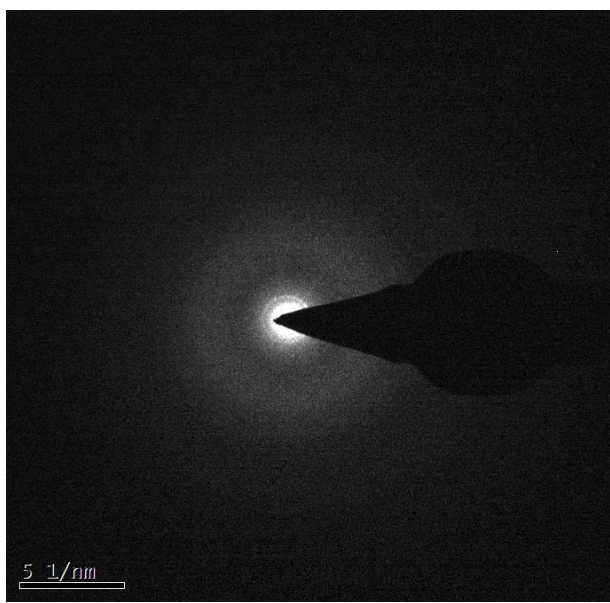


Figure 2. The SEM images of the $\text{Ti}/\text{Ru}_{0.4}\text{Sn}_{0.6}\text{O}_2$ electrode.



(a)



(b)

Figure 3. The HRTEM and SAD images of the electrode.

beneficial for supercapacitor application because it can be rearranged when ions such as H^+ and OH^- are inserted while the lattice of crystalline is rigid and is difficult to expand. But in this paper not the absolute amorphism but the very poorly crystalline is in favor of the capacitance.

3.4. Electrochemical Properties

The charge-discharge potential windows play an important role for supercapacitor performance. **Figure 4** shows the CV curves of the electrodes at 25 mv/s scan rate with different potential ranges. It's seen that different poten-

tial ranges have almost similar curve shapes. The cyclic voltammograms are almost rectangular and symmetrical. This indicates that the oxidation and reduction processes at the electrode interface are highly reversible. Every curve exhibited a capacitive behavior. We also can observe the response current of the electrode almost reverses instantaneously when the scan direction changes whether from anodic to cathodic scan or from cathodic to anodic scan. The changes exhibit almost vertical lines which reflect little impedance of the electrodes [5].

The specific capacitance (C_{sp}) of the $Ti/Ru_{0.4}Sn_{0.6}O_2$ electrode is obtained to explore the dependence of the electrodes' specific capacitance on the potential ranges. **Table 1** shows the values of specific capacitance. The C_{sp} of the $Ti/Ru_{0.4}Sn_{0.6}O_2$ electrode obtained from $Q/(2\Delta V \cdot W)$, where Q is the CV charge, ΔV is the potential range of CV and W is the weight of ruthenium oxides. The C_{sp} of the electrodes increases with the broadened potential window. The increase in capacitance at broader windows is attributed to the presence of inner active sites, which can involve in the redox transitions completely, probably due to the diffusion effect of proton within the electrode [10]. The increasing trend of the capacitance suggests that the parts of the surface of electrode are accessible at high charging-discharging rate. Hence, the specific capacitance obtained at the broadest window is believed to be close to that of full utilization of the electrode material.

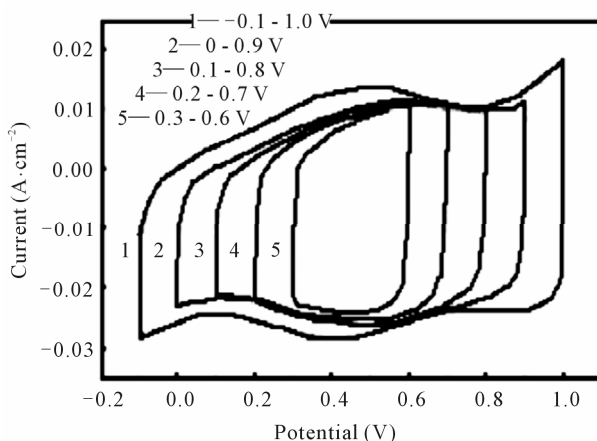


Figure 4. Cyclic voltammogram of the $Ti/Ru_{0.4}Sn_{0.6}O_2$ electrode at different potential windows.

Table 1. The specific capacitance of the $Ti/Ru_{0.4}Sn_{0.6}O_2$ electrode at different potential ranges.

Potential ranges (V vs SCE)	0.3 - 0.6	0.2 - 0.7	0.1 - 0.8	0 - 0.9	-0.1 - 1.0
C_s, RuO_2 ($F \cdot g^{-1}$)	552	580	577	576	648

Compared with the CV experiment, the galvanostatic charge-discharge experiment can further reflect the supercapacitance characteristics. **Figure 5** shows the galvanostatic charge-discharge curve of Ti/Ru_{0.4}Sn_{0.6}O₂ electrodes at different current densities. The curves show linear change with the time changing and exhibit good capacitance characteristics. The charge curve and the discharge curve are symmetrical, which show a better reversibility. With current density increasing, the discharge time of the electrodes shortens, and the corresponding specific capacitance also decreases gradually. The reason is the charge-discharge process is related with not only the moving speed of ions in the electrolyte, but also the adsorption process on the electrode surface. In a smaller current density, ion moving speed and adsorption process is developed completely. So the electrode reaction not only occurs in the electrode surface, but occurs in body phases. The active sites in the electrode are fully utilized, which lead to the charge-discharge process completely. Similar results have been reported [12].

Figure 6 shows the relationship between cycle number and specific capacitance of the Ti/Ru_{0.4}Sn_{0.6}O₂ electrode in 0.5 mol/L H₂SO₄ at the scan rate of 25 mV/s and the potential window of -0.1 - 1.0 V. The specific capacitance decreases gradually with increasing cycle number. The specific capacitance declines about 18.8% after 1000 scan cycles. This suggests that the electrode has a good stability and is useful for supercapacitor application.

4. Conclusions

The electrodes with poorly crystalline Ru_{0.4}Sn_{0.6}O₂ solid solution coated on Ti substrate have been prepared by 260°C thermal decomposition. The morphological study shows that the electrodes have mud-cracks structure with cracks 0.2 μm in width. The electrode has stable electro-

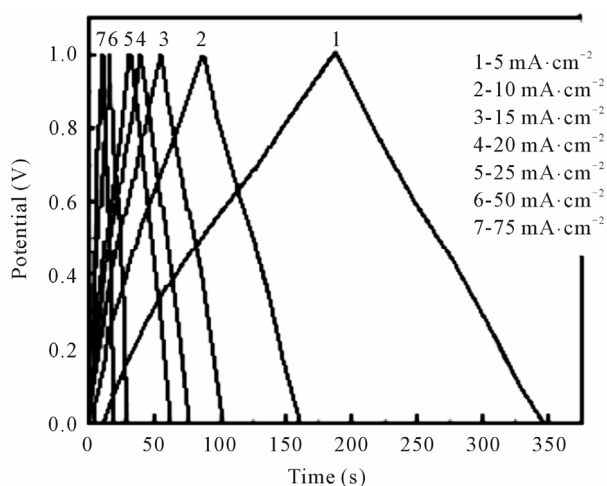


Figure 5. Galvanostatic charge/discharge of the Ti/Ru_{0.4}Sn_{0.6}O₂ electrode at different current densities.

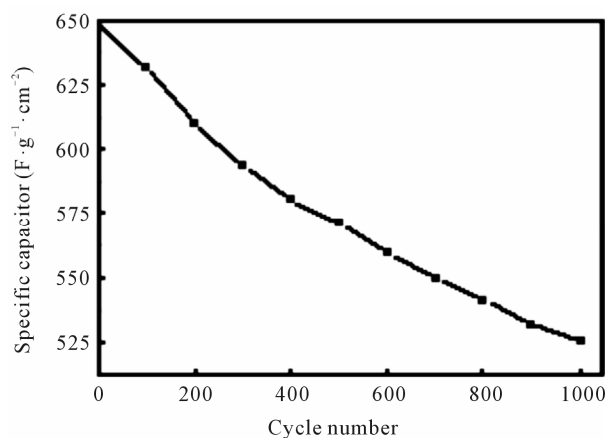


Figure 6. Relationship between cycle number and specific capacitance of the Ti/Ru_{0.4}Sn_{0.6}O₂ electrode in 0.5 mol/L H₂SO₄.

chemical capacitor properties with a maximum specific capacitance of 648 F/g within a scan potential window -0.1 - 1.0 V in 0.5 M H₂SO₄ electrolyte solution. Thus the electrode is found to be useful for high capacity electrochemical supercapacitor application.

5. Acknowledgements

The financial support of Natural Science Foundation of Fujian Province of China (2009J01239) is gratefully acknowledged.

REFERENCES

- [1] R. E. Conway, "Electrochemical Supercapacitors: Scientific Fundamentals and Technical Applications," Kluwer Academic, Plenum Publishers, New York, 1999.
- [2] X. Pang, Z. Ma and L. Zuo, "Research Progress in Electrode Materials for Supercapacitor Used Metal Oxides," *Surface Technology*, Vol. 38, No. 3, 2009, pp. 77-82.
- [3] S. Sarangapani, "Materials for Electrochemical Capacitors," *Journal of the Electrochemical Society*, Vol. 143, No. 11, 1996, pp. 3791-3799. [doi:10.1149/1.1837291](https://doi.org/10.1149/1.1837291)
- [4] K. H. Chang and C. C. Hu, "Hydrothermal Synthesis of Binary Ru-Ti Oxides with Excellent Performances for Supercapacitors," *Electrochimica Acta*, Vol. 52, No. 4, 2006, pp. 1749-1757. [doi:10.1016/j.electacta.2006.01.076](https://doi.org/10.1016/j.electacta.2006.01.076)
- [5] R. Kötz and M. Carlen, "Principles and Applications of Electrochemical Capacitors," *Electrochimica Acta*, Vol. 45, No. 15-16, 2000, pp. 2483-2498. [doi:10.1016/S0013-4686\(00\)00354-6](https://doi.org/10.1016/S0013-4686(00)00354-6)
- [6] V. D. Patake, S. M. Pawar, V. R. Shinde, *et al.*, "The Growth Mechanism and Supercapacitor Study of Anodically Deposited Amorphous Ruthenium Oxide Films," *Current Applied Physics*, Vol. 10, No. 1, 2010, pp. 99-103. [doi:10.1016/j.cap.2009.05.003](https://doi.org/10.1016/j.cap.2009.05.003)
- [7] H.-R. Chen, H.-H. Lai and J.-J. Jow, "Annealing Effect on the Performance of RuO₂-Ta₂O₅/Ti Electrodes for Use

- in Supercapacitors,” *Materials Chemistry and Physics*, Vol. 125, No. 3, 2011, pp. 652-655.
[doi:10.1016/j.matchemphys.2010.10.003](https://doi.org/10.1016/j.matchemphys.2010.10.003)
- [8] Y.-Y. Liang, L. H. Lin and X.-G. Zhang, “Solid State Synthesis of Hydrous Ruthenium Oxide for Supercapacitors,” *Journal of Power Sources*, Vol. 173, No. 1, 2007, pp. 599-605. [doi:10.1016/j.jpowsour.2007.08.010](https://doi.org/10.1016/j.jpowsour.2007.08.010)
- [9] H.-Q. Li, Y. Zou and Y.-Y. Xia, “A Study of Nitroxide Polyradical/Activated Carbon Composite as the Positive Electrode Material for Electrochemical Hybrid Capacitor,” *Electrochim Acta*, Vol. 52, No. 5, 2007, pp. 2153-2157. [doi:10.1016/j.electacta.2006.08.031](https://doi.org/10.1016/j.electacta.2006.08.031)
- [10] J. Wen, X. Ruan and Z. Zhou, “Preparation and Electrochemical Performance of Novel Ruthenium-Manganese Oxide Electrode Materials for Electrochemical Capacitors,” *Journal of Physics and Chemistry of Solids*, Vol. 70, No. 5, 2009, pp. 816-820. [doi:10.1016/j.jpics.2009.03.015](https://doi.org/10.1016/j.jpics.2009.03.015)
- [11] W. Zhang, K. Liu, Y. Zhang, et al., “Studies of Charge-Discharge Process in MnO₂ Supercapacitor,” *Chemistry*, Vol. 70, No. 3, 2007, pp. 217-221.
- [12] Y. Chen, W. Zhang and Z. Zhang, “Effect of Additive Doping on Electrochemical Performance of Hydrothermal Prepared MnO₂,” *Chinese Journal of Power Sources*, Vol. 33, No. 8, 2009, pp. 673-678.
- [13] Y. Chen, W. Zhang and Z. Zhang, “Molten Salt Synthesis and Electrochemical Properties of Manganese Dioxide,” *Fine Chemical*, Vol. 26, No. 2, 2009, pp. 115-118.
- [14] Y. Feng, M. Zhang, Y. Chen, et al., “Preparation and Electrochemical Performance of Cr Doped MnO₂,” *The Chinese Journal of Nonferrous Metals*, Vol. 15, No. 2, 2005, pp. 316-320.
- [15] A. Yuan and Q. Zhang, “Solid Reaction Preparation and Electrochemical Characteristics of Nano-Structured Co₃O₄ Material for Supercapacitor,” *Journal of Functional Materials and Devices*, Vol. 13, No. 1, 2007, pp. 1-6.
- [16] X. Wang, Y. Ou and A. Kemu, “Supercapacitor Characteristics of Co(OH)₂ Synthesized by Hydrothermal Synthesis,” *Natural Science Edition*, Yili Normal University, Vol. 4, 2009, pp. 20-22.
- [17] M. L. Zhang and Z. X. Liu, “Supercapacitor Characteristics of Co(OH)₂ Synthesized by Deposition Transformation,” *Chinese Journal of Inorganic Chemistry*, Vol. 18, No. 5, 2002, pp. 513-517.
- [18] Y. Chen, L. Liu and Z. Zhang, “Preparation of NiO by Parallel Flow Precipitation Process and Its Capacitance Performance,” *Fine Chemicals*, Vol. 25, No. 5, 2002, pp. 424-427.
- [19] Z. Yu, Y. Dai and W. Chen, “Preparation and Electrochemical Properties of Nanostructured Flower-Like NiO by Hydrothermal-Decomposition,” *Journal of Xihua University*, Vol. 29, No. 1, 2010, pp. 99-103.
- [20] C.-C. Hu, K.-H. Chang and C.-C. Wang, “Two-Step Hydrothermal Synthesis of Ru-Sn Oxide Composites for Electrochemical Supercapacitors,” *Electrochimica Acta*, Vol. 52, 2007, pp. 4411-4418.
[doi:10.1016/j.electacta.2006.12.022](https://doi.org/10.1016/j.electacta.2006.12.022)